DALTON
FULL PAPER

Out-of-plane dimers of Mn(III) quadridentate Schiff-base complexes with saltmen^{2-} and naphtmen^{2-} ligands: structure analysis and ferromagnetic exchange

Hitoshi Miyasaka,*[a] Rodolphe Clérac,*[b] Tomohiko Ishii,[a] Ho-Chol Chang,[c] Susumu Kitagawa[c] and Masahiro Yamashita[a]

[a] *Department of Chemistry, Graduate School of Science, Tokyo Metropolitan University, 1-1 Minami-Ohsawa, Hachioji, Tokyo 192-0397, Japan*
[b] *Centre de Recherche Paul Pascal, CNRS UPR 8641, Avenue du Dr. Schweitzer, 33600 Pessac, France*
[c] *Department of Synthetic Chemistry and Biological Chemistry, Faculty of Engineering, Kyoto University, Yoshida, Sakyo-ku, Kyoto 606-8501, Japan*

Received 4th December 2001, Accepted 24th January 2002
First published as an Advance Article on the web 11th March 2002

Six Mn(III) quadridentate Schiff base compounds with *N*,*N*′-(1,1,2,2-tetramethylethylene)bis(salicylideneiminato) dianion (saltmen^{2-}) and *N*,*N*′-(1,1,2,2-tetramethylethylene)bis(naphthylideneiminato) dianion (naphtmen^{2-}) have been prepared and structurally characterized: [Mn(saltmen)(H_2O)]ClO_4 (**1**), [Mn(naphtmen)(H_2O)]ClO_4 (**2**), [Mn(saltmen)(NCS)] (**3**), [Mn(naphtmen)(NCS)] (**4**), [Mn(saltmen)(Cl)] (**5**) and [Mn(naphtmen)(Cl)] (**6**). Among them, **1** and **2** form phenolate-bridged out-of-plane dimers with Mn–$O_{phenolate}$ bond distances of 2.434(2) and 2.662(3) Å, respectively. X-Ray diffraction analysis shows that compounds **3**, **4** and **6** can also be considered as out-of-plane dimers in spite of long Mn–$O_{phenolate}$ interacting distances (3.441(2) Å for **3**, 3.758(3) Å for **4** and 3.505(5) Å for **6**). In contrast with the above compounds, **5** is a discrete Mn(III) mononuclear complex with a square-pyramidal geometry. In the dimer series (compounds **1**–**4** and **6**), the out-of-plane intermolecular distance varies dramatically according to equatorial ligands, saltmen^{2-} or naphtmen^{2-}, and axial ligands, H_2O, NCS^- and Cl^-. The relation between substitution of the ligands and structural parameters of the dimeric molecules are discussed. Magnetic susceptibility studies reveal interesting intra-dimer ferromagnetic interactions between Mn(III) ions. Our work reports on these new $S = 4$ building blocks that open new possibilities in the design of magnetic molecule-based materials.

Introduction

Exchange interaction between paramagnetic centers of a large number of poly-metal complexes has already been investigated. The nature and the tuning of magnetic interactions between metal centers are crucial points in the conception of molecule-based magnetic materials.[1] The family of manganese(III) salen-type Schiff base compounds is one of the most appealing candidates as a building paramagnetic motif for multi-dimensional expanded structures. It could provide not only a relevant coordinating link but also an interesting high-spin ground state due to the Mn(III) ion (S = 2).[2] Although the simplest motif is a monomeric form [Mn(L)(H_2O)(S)]$^+$ (**A**), a dimeric form [$Mn_2(L)_2(H_2O)_2$]$^{2+}$ (**B**) (L = salen-type Schiff base ligand, S = unidentate solvent ligand)[3] is also available for elaborating new systems.[2b] In some cases, the **B** form exhibits ferromagnetic intra-dimer interaction, affording an unsual $S = 4$ ground spin state. This peculiarity gives to the **B** form an appealing property for a building block to design new magnetic materials.

Numerous dimeric manganese(III) compounds with salen-type ligands **C** (shown in Chart 1) exhibiting antiferromagnetic intra-dimer interaction, have been published in the literature.[4–10,11] In contrast, reports on the ferromagnetic dimers ($S = 4$) are still sparse,[2b,12–14] indicating the difficulty to control magnetic interaction between manganese(III) ions in [$Mn_2(L)_2(H_2O)_2$]$^{2+}$ units. We present here the synthesis of five out-of-plane dimeric compounds which display ferromagnetic intra-dimer interaction: [Mn(saltmen)(H_2O)]ClO_4 (**1**), [Mn(naphtmen)(H_2O)]ClO_4 (**2**), [Mn(saltmen)(NCS)] (**3**), [Mn(naphtmen)(NCS)] (**4**), and [Mn(naphtmen)(Cl)] (**6**) (where saltmen^{2-} **D** is *N*,*N*′-(1,1,2,2-tetramethylethylene)bis(salicylideneiminate) and naphtmen^{2-} **E** is *N*,*N*′-(1,1,2,2-tetramethylethylene)bis(naphthylideneiminate). In addition, it is worth noticing that it is also possible to synthesize monomeric compounds, [Mn(saltmen)(Cl)] (**5**), depending on the apical

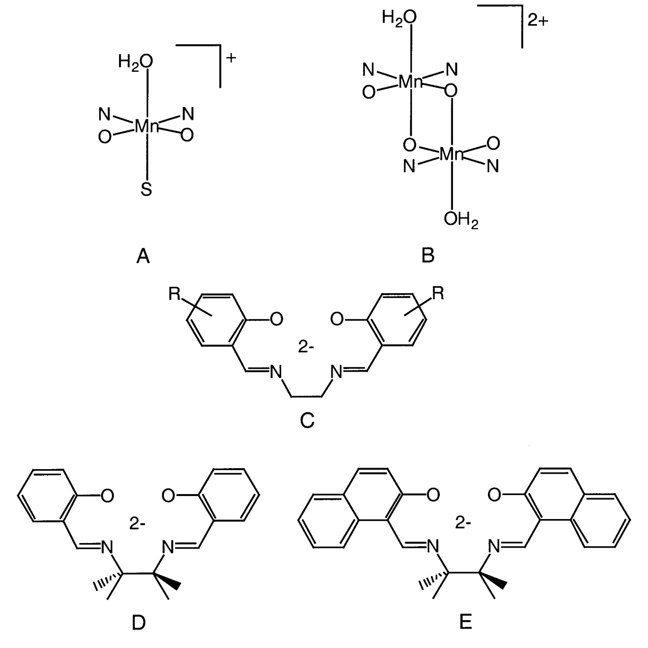

Chart 1

ligands used. Crystal structures in relation with the magnetic properties of compounds **1**–**6** will be discussed in this report.

Experimental

General procedures and materials

All chemicals and solvents used during the synthesis were reagent grade. The H_2saltmen and H_2naphtmen were synthesized by mixing 1,1,2,2-tetramethylethylenediamine with salicylaldehyde or naphthylaldehyde in a 1 : 2 molar ratio in ethanol. **CAUTION:** Perchlorate salts are potentially explosive and should only be handled in small quantities.

Syntheses

Preparation of [Mn(saltmen)(H_2O)]ClO_4 (1). A methanol solution (20 cm^3) of manganese(III) acetate dihydrate (1.34 g, 5 mmol) was added to a methanol solution (50 cm^3) of the Schiff base ligand H_2saltmen (1.62 g, 5 mmol). After heating the brown solution at 50 °C and stirring for 30 min, sodium perchlorate (610 mg, 5 mmol) was added. Before filtration, 80 cm^3 of hot water was added to the resulting hot solution. The filtrate was left to stand for one week at room temperature. Dark brown crystals were collected by suction filtration, washed with a minimum amount of water and dried *in vacuo*. Anal. Calc. for $C_{20}H_{24}N_2O_7ClMn$: C, 48.55; H, 4.89; N, 5.66. Found: C, 48.32; H, 4.96; N, 5.60%. IR(KBr): ν(C=N), 1601 cm^{-1}; ν(Cl–O), 1080, 1120, 1140 cm^{-1}.

Preparation of [Mn(naphtmen)(H_2O)]ClO_4 (2). The same preparation as that presented for **1** was used for **2** using H_2naphtmen instead of H_2saltmen. For **2**·MeOH, Anal. Calc. for $C_{29}H_{32}N_2O_8ClMn$: C, 55.56; H, 5.14; N, 4.47. Found: C, 55.46; H, 5.14; N, 4.48%. IR(KBr): ν(C=N), 1587–1620 cm^{-1}; ν(Cl–O), 1060, 1080, 1100, 1120 cm^{-1}.

Preparation of [Mn(saltmen)(NCS)] (3). Solid sodium thiocyanate (81 mg, **1** mmol) was added to a methanol solution (30 cm^3) of **1** (495 mg, 1 mmol). The resulting brown solution was stirred at room temperature for 30 min. During this time, brown microcrystals precipitated. These crystals were collected by suction filtration, washed with a minimum amount of methanol and dried *in vacuo*. Recrystallization was performed in order to obtain large crystals in chloroform–ethanol solution. Anal. Calc. for $C_{21}H_{22}N_3O_2SMn$: C, 57.93; H, 5.09; N, 9.65. Found: C, 57.53; H, 5.09; N, 9.65%. IR(KBr): ν(NCS), 2062 cm^{-1}; ν(C=N), 1605 cm^{-1}.

Preparation of [Mn(naphtmen)(NCS)] (4). The synthetic procedure for **4** is similar to that presented for **3**, replacing H_2naphtmen with H_2saltmen. Anal. Calc. for $C_{29}H_{26}N_3O_2SMn$: C, 65.04; H, 4.89; N, 7.85. Found: C, 64.65; H, 4.95; N, 7.78%. IR(KBr): ν(NCS), 2062 cm^{-1}; ν(C=N), 1618, 1597, 1586 cm^{-1}.

Preparation of [Mn(saltmen)(Cl)] (5). Triethylamine (506 mg, 5mmol) was first added to a methanol solution (50 cm^3) of H_2saltmen (1.62 g, 5 mmol). In a second step, a methanol solution (20 cm^3) of manganese(II) chloride (629 mg, 5 mmol) was then added to the resulting solution. After heating and stirring for 1 h at 50 °C, 80 cm^3 of hot water was added to the brown solution before filtration. The filtrate was left to stand for one week at room temperature. Obtained dark brown crystals were collected by suction filtration, washed with a minimum amount of water and dried *in vacuo*. Anal. Calc. for $C_{20}H_{22}N_2O_2ClMn$: C, 58.19; H, 5.37; N, 6.79. Found: C, 57.82; H, 5.32; N, 6.76. IR(KBr): ν(C=N), 1601 cm^{-1}.

Preparation of [Mn(naphtmen)(Cl)] (6). The synthetic procedure for **6** is similar to that described for **5**, replacing H_2naphtmen with H_2saltmen. For **6**·H_2O, Anal. Calc. for $C_{28}H_{28}N_2O_3ClMn$: C, 63.34; H, 5.32; N, 5.32. Found: C, 63.71; H, 5.17; N, 5.20%. IR(KBr): ν(C=N), 1617, 1599, 1586 cm^{-1}.

Physical measurements

Infrared spectra were measured on KBr disks with a Hitachi I-5040FT-IR spectrophotometer. Magnetic susceptibility data were obtained over the temperature range from 1.8 to 300 K at 0.1 T using an MPMS-XL SQUID susceptometer (Quantum Design, Inc.). Field dependencies of magnetization up to 5.5 T were studied on the same susceptometer. Samples for magnetic measurements were ground into powder in order to avoid an effect of the magnetic anisotropy.[11] Corrections were applied for diamagnetism using Pascal's constants[15] and for sample holders. χ is defined as the magnetic susceptibility (M/H) per manganese(III) ion.

X-Ray data collection, reduction, and structure determination

Measurements for **1** and **2** were made on a Rigaku AFC7R diffractometer with graphite monochromated Mo-Kα radiation ($\lambda = 0.71069$ Å) and a 12 kW rotating anode generator. The data were collected at a temperature of 23 ± 1 °C using the ω–2θ scan technique to a maximum 2θ value of 55.0° at an average scan speed of 4.0° min^{-1} (in ω). The weak reflections ($I < 10.0\sigma(I)$) were rescanned (maximum of 5 scans), and the counts were accumulated to ensure good counting statistics. Stationary background counts were recorded on each side of reflections; 5264 and 6726 reflections were collected for **1** and **2**, respectively. Measurements for **3** and **4** were made on a Rigaku CCD diffractometer with graphite monochromated Mo-Kα radiation ($\lambda = 0.71069$ Å); 14364 and 5821 reflections were collected at 20 ± 1 °C for **3** and **4**, respectively. Measurements for **5** and **6** were made on a Rigaku Imaging plate diffractometer with graphite monochromated Mo-Kα radiation ($\lambda = 0.71069$ Å); 34410 and 11145 reflections were collected at −100 ± 1 °C for **5** and **6**, respectively.

The structures for **1**–**6** were solved by direct methods (SIR92, PATTY, SHELX97)[16] and expanded using Fourier techniques.[17] The non-hydrogen atoms were refined anisotropically, while hydrogen atoms were introduced as fixed contributors. Full-matrix least-squares refinements based on all data of unique reflections and the data with $I > 2.00\sigma(I)$ were employed (unweighted and weighted agreement factors of $R = \Sigma||F_o| - |F_c||/\Sigma|F_o|$, ($I > 2.00\sigma(I)$) and $R_w = [\Sigma w(F_o^2 - F_c^2)^2/\Sigma w(F_o^2)^2]^{1/2}$, (all data) were used). All calculations were performed using the teXsan crystallographic software package of the Molecular Structure Corporation.[18] Crystal data and details of the structure determinations for **1**–**6** are summarized in Table 1.

CCDC reference numbers 168755–168760.

See http://www.rsc.org/suppdata/dt/b1/b111094m/ for crystallographic data in CIF or other electronic format.

Results and discussion

Structure descriptions of out-of-plane dimers

All compounds **1**–**6** can be simply described as [Mn(L^n)(X)]$^{0/+1}$ on the basis of one Mn(III) ion. [Mn(L^n)(X)]$^{0/+1}$ units are composed of an Mn(III) ion surrounded by the quadridentate Schiff base ligand (L^1 = saltmen^{2-} or L^2 = naphtmen^{2-}) and one axial ligand (X = H_2O, NCS^-, Cl^-). These compounds can be classified to three types according to "dimerization" distances. Type I corresponds to out-of-plane dimers with relatively short Mn ··· O* *bonding* distances, (where the O* atom refers to the phenolate oxygen atom of the another [Mn(L^n)(X)]$^{0/+1}$ unit in out-of-plane dimeric fashion). Type II includes out-of-plane dimers with long Mn ··· O* distances (weak interaction). Type III corresponds to monomers with square-pyramidal coordination geometry.

Table 1 Crystallographic information for **1**–**6**

	1 (dimer)	**2**·MeOH (dimer)	**3**	**4**	**5**	**6**
Formula	$C_{40}H_{48}N_4O_{14}Cl_2Mn_2$	$C_{58}H_{64}N_4O_{16}Cl_2Mn_2$	$C_{21}H_{22}N_3O_2SMn$	$C_{29}H_{26}N_3O_2SMn$	$C_{20}H_{22}N_2O_2ClMn$	$C_{28}H_{26}N_2O_2ClMn$
M	989.62	1253.94	435.42	535.54	412.80	512.92
Space group	$P2_1/a$ (no. 14)	$P\bar{1}$ (no. 2)	$P2_1/c$ (no. 14)	$P2_1/a$ (no. 14)	$P2_12_12_1$ (no. 19)	$P2_1/c$ (no. 14)
T/°C	23 ± 1	23 ± 1	20 ± 1	20 ± 1	−100 ± 1	−120 ± 1
λ/Å	0.71069	0.71069	0.71069	0.71069	0.71069	0.71069
a/Å	20.830(1)	13.360(8)	8.2800(6)	14.2464(3)	20.1584(5)	13.481(3)
b/Å	13.596(1)	13.76(1)	19.873(2)	13.1533(6)	21.9138(5)	12.266(1)
c/Å	7.526(1)	8.463(6)	12.1163(3)	14.3675(3)	8.6859(2)	14.388(3)
α/°	90	101.76(7)	90	90	90	90
β/°	89.818(8)	94.45(7)	95.7988(6)	109.6759(5)	90	97.754(3)
γ/°	90	112.93(5)	90	90	90	90
V/Å^3	2131.3(3)	1381(1)	1983.5(2)	2535.1(1)	3836.9(2)	2357.4(8)
Z	2	1	4	4	8	4
D_c/g cm^{-3}	1.542	1.507	1.458	1.403	1.429	1.445
F_{000}	1024.00	652.00	904.00	1112.00	1712.00	1064.00
μ(Mo-Kα)/cm^{-1}	7.90	6.30	7.93	6.35	8.43	7.02
GOF	1.29	1.95	1.68	1.73	0.57	1.20
Unique refl.	4900	6299	4354	5821	4931	4698
No. of refl. used ($I > 2.00\sigma(I)$)	2859	4408	3406	4245	2982	2371
R^a ($I > 2.00\sigma(I)$)	0.048	0.070	0.042	0.063	0.032	0.099
$R_w^{b,c}$ (all data)	0.138	0.203	0.138	0.182	0.078	0.235

[a] $R = \Sigma||F_o| - |F_c||/\Sigma|F_o|$ ($I > 2.00\sigma(I)$). [b] $R_w = [\Sigma w(F_o^2 - F_c^2)^2/\Sigma w(F_o^2)^2]^{1/2}$ (all data). [c] $w = [\sigma_c^2(F_o^2) + (p(\mathrm{Max}(F_o^2, 0) + 2F_c^2)/3)^2]^{-1}$ ($\sigma_c(F_o^2)$ = e.s.d. based on counting statistics; p = p-factor, 0.042 for **1**; 0.059 for **2**; 0.050 for **3**; 0.070 for **4**; 0.047 for **5**, 0.082 for **6**).

Compounds **1** and **2** belong to the type I classification. ORTEP drawings of the cationic parts of **1** and **2** are depicted in Fig. 1(a) and (b), respectively. Both structures have an inversion center at the midpoint of the Mn ··· Mn vector. The characteristic bond distances and angles of the dimeric core for **1** and **2** are: Mn–Mn* 3.381(1), 3.541(1) Å, Mn–O(1) (O(1): intramolecular phenolate oxygen) 1.909(2), 1.896(3) Å, Mn–O(1)* (O(1)*: intermolecular phenolate oxygen) 2.434(2), 2.662(3) Å, Mn–O(1)*–Mn* 101.58(10), 100.6(1)°, O(1)–Mn–O(1)* 78.42(10), 79.4(1)°, respectively (*; 1 − x, −y, −z for **1**, −x, −y, −z for **2**). The apical positions of the Mn(III) ion are occupied by a phenolate oxygen atom, O(1)*, of the neighboring $[\mathrm{Mn(L''})(H_2O)]^+$ unit and a water oxygen atom, O(3), with Mn–O(3) 2.261(3) and 2.224(3) Å for **1** and **2**, respectively. Globally, the Mn(III) coordination sphere adopts a distorted square bipyramidal geometry due to the Jahn–Teller distortion induced by the quadridentate Schiff base type ligand.

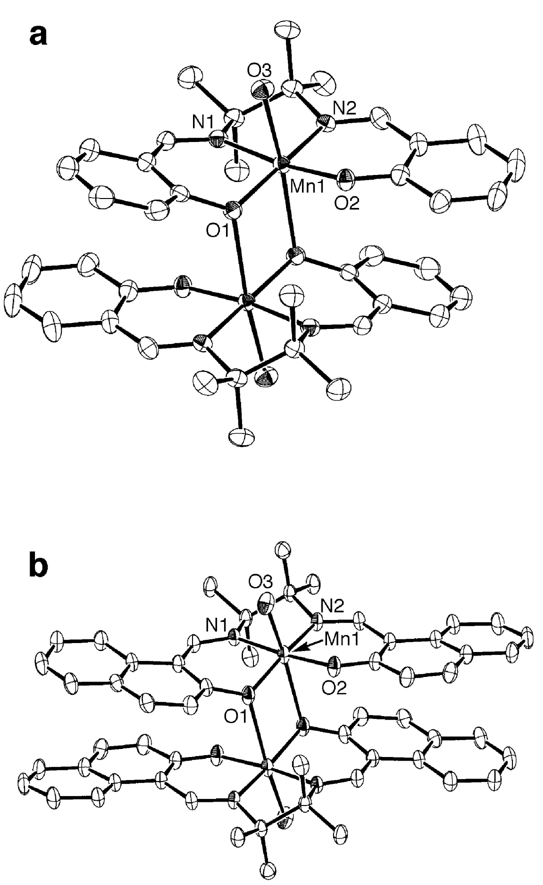

Fig. 1 ORTEP drawings of the cationic out-of-plane dimer $[\mathrm{Mn(saltmen)}(H_2O)]^+$ (**1**) (a) and $[\mathrm{Mn(naphtmen)}(H_2O)]^+$ (**2**) (b) with the atom numbering scheme of the unique atoms (30% probability ellipsoids). Hydrogen atoms are omitted for clarity.

On the other hand, compounds **3**, **4** and **6** belong to our type II classification. ORTEP drawings of **3**, **4** and **6** are depicted in Fig. 2(a), (b) and (c), respectively. The Mn(III) atom in these compounds assumes a Jahn–Teller distorted square bipyramidal geometry. One apical site is occupied by a nitrogen atom of thiocyanate anion (NCS^-) with Mn–N(3) 2.151(3) Å for **3** and 2.096(3) Å for **4**. The other apical site of Mn(III) ion has a weak interaction with a phenolate oxygen of the neighboring [Mn(L″)(NCS)] unit with Mn–O(2)* 3.441(2) Å for **3** and 3.758(3) Å for **4** (*; 1 − x, −y, 1 − z for **3**, 2 − x, 1 − y, −z for **4**). As weak as this Mn–O(2)* interaction is, the structure motif can still be considered as an out-of-plane dimer. For **6**, one apical site of Mn(III) ion is occupied by a chloride anion with Mn–Cl(1) 2.383(2) Å. As well as **3** and **4**, the other apical site interacts with a phenolate oxygen of a neighboring [Mn(L″)(Cl)] unit in out-of-plane fashion with Mn–O(2)* 3.505(5) Å (*; 1 − x, −y, 1 − z for **6**). Interestingly, it is worth noting that the use of stronger donor ligands (NCS^- and Cl^-) than water (**1** and **2**), leads to shorter bond distances between the Mn(III) and apical ligands (Mn–NCS and Mn–Cl compared to Mn–OH_2). Consequently, the other apical bond Mn–O (where O is a phenolate oxygen of a neighboring [Mn(L″)(X)] unit) is weakened in **3**, **4** and **6** compared to **1** and **2**.

Structure description of monomeric compound 5

The only compound of type III found in our study, is **5** which crystallized in the acentric space group $P2_12_12_1$. The two independent molecules present in the structure are almost structurally identical. Their ORTEP drawing is depicted in Fig. 3. The Mn(III) atoms assume a distorted square pyramidal geometry, in which the apical site is occupied by chloride

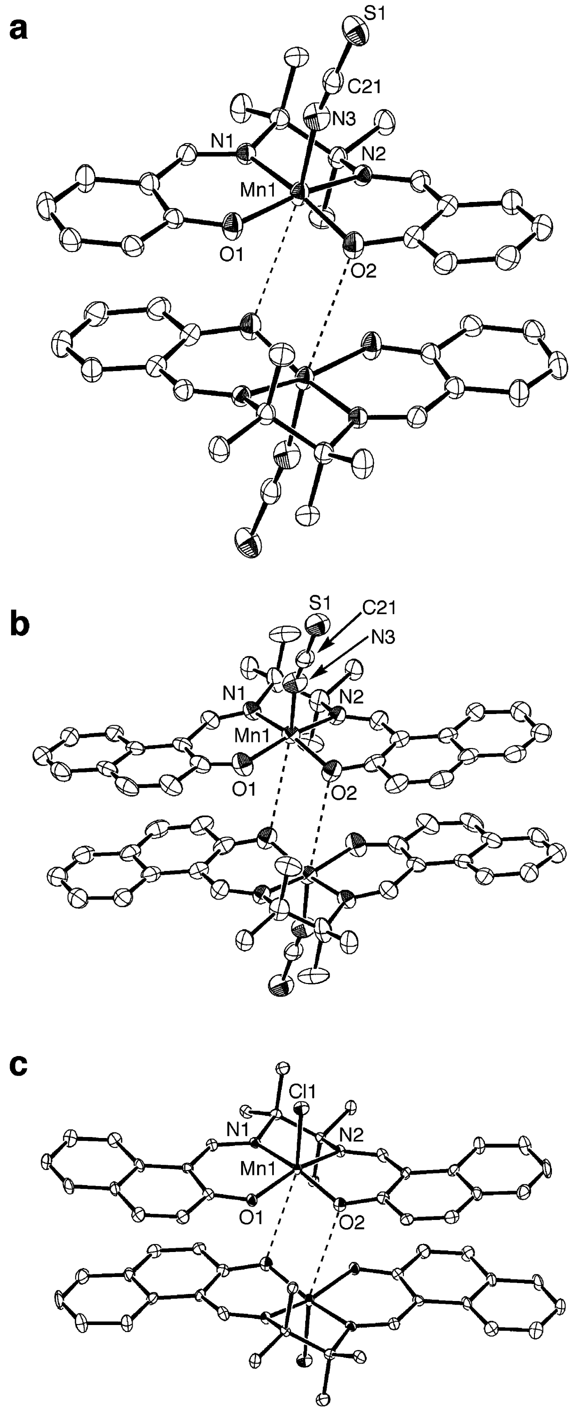

Fig. 2 ORTEP drawings of the out-of-plane dimers [Mn(saltmen)(NCS)] (**3**) (a), [Mn(naphtmen)(NCS)] (**4**) (b) and [Mn(naphtmen)(Cl)] (**6**) (c) with the atom numbering scheme of the unique atoms (30% probability ellipsoids). Hydrogen atoms are omitted for clarity.

anion (Cl^-) with Mn(1)–Cl(1) 2.356(1) Å and Mn(2)–Cl(2) 2.397(1) Å. The nearest intermolecular Mn ··· Mn distance is 6.96 Å.

Magnetic properties of 1–6

The temperature-dependence of the magnetic susceptibility of **1**–**6** was measured on ground polycrystalline samples in the temperature range 1.8 to 300 K under 1000 G. χT *vs.* T plots of **1**–**4** and **6** are shown in Fig. 4. χT values for these compounds at room temperature are in the range of 2.9–3.2 cm^3 K mol^{-1} (per Mn(III) ion). These values are compatible with 3.0 cm^3 K mol^{-1} of a high-spin Mn(III) $S_{Mn} = 2$ ion calculated assuming g_{Mn} =

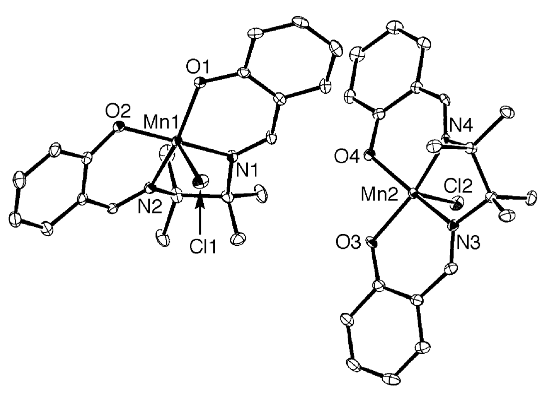

Fig. 3 ORTEP drawing of [Mn(saltmen)(Cl)] (**5**) with the atom numbering scheme of the unique atoms (30% probability ellipsoids). Hydrogen atoms are omitted for clarity.

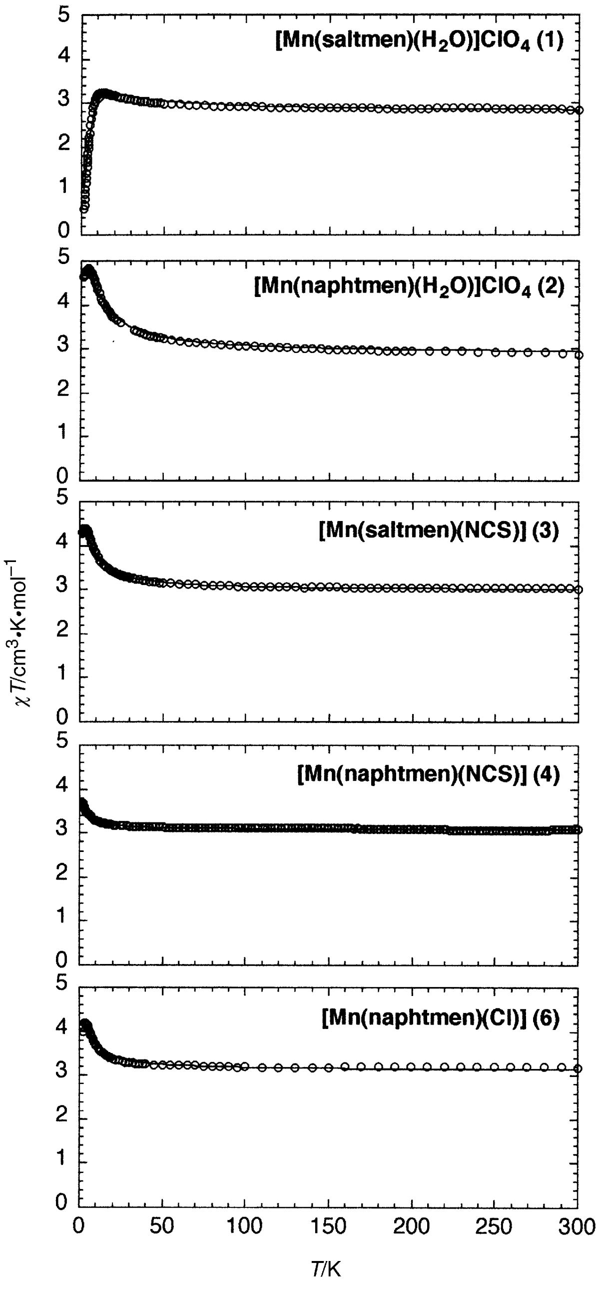

Fig. 4 χT *vs.* T plots of **1**–**4** and **6** measured under 0.1 T. Solid lines represent the best fits of the data using the parameters summarized in Table 2.

2.0. For all compounds, the χT value increases gradually upon lowering temperature to reach a maximum. A slight decrease of χT is observed at low temperature in **1**, **2**, **3** and **6**. The decrease at low temperature could be associated with principally two phenomena: the zero-field splitting (ZFS) arising from Mn(III) ion and/or possible intermolecular antiferromagnetic interaction between the neighboring dimer units. As shown in Fig. 5(a), the magnetization curve at 1.8 K for **1** presents a sigmoidal shape which could be attributed to the transition from an antiferromagnetic to a spin-flop state. The spin-flop field is estimated to be at the inflexion point around 1 T (maximum of the derivative, see Fig. 5(a)). This antiferromagnetic behavior is confirmed by the temperature dependence of the magnetic susceptibility between 1.8 and 7 K at different fields (Fig. 5(b)). As expected the susceptibility is field independent in the paramagnetic phase above 5 K. Below this temperature, the susceptibility become field dependent, which is characteristic of the occurrence of the antiferromagnetic ground state with T_N = 5 K. This result clearly indicates that inter-dimer antiferromagnetic interaction in **1** are significant. This is also confirmed from the structural point of view, shorter inter-dimer distances in structural packing (the nearest inter-dimer Mn ··· Mn distance is 5.59 Å for **1**) are observed in comparison with those in the other compounds (7.85–8.28 Å). As expected in regard to these inter-dimer distances, no antiferromagnetic state is observed in compounds **2**–**4** and **6**.

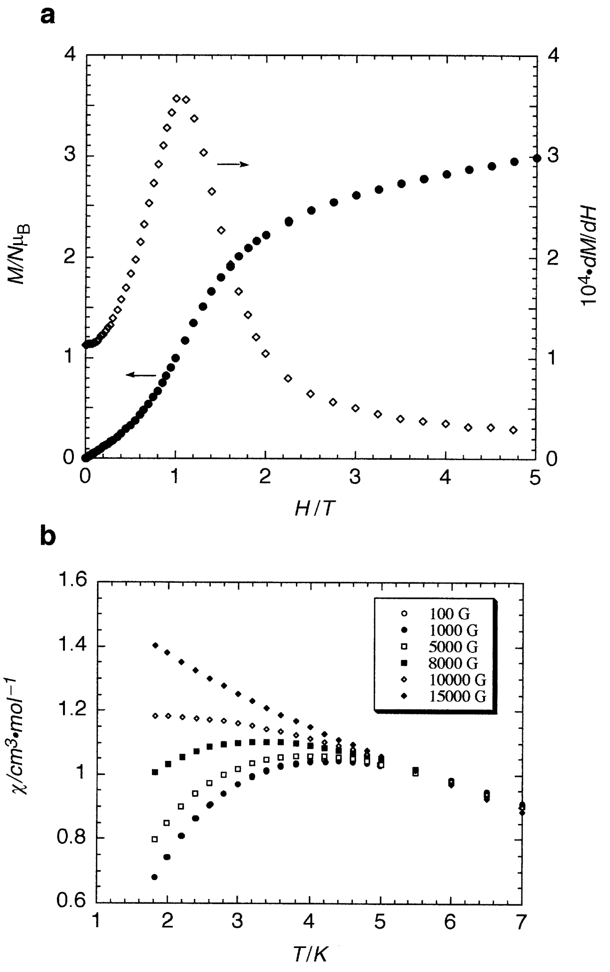

Fig. 5 (a) Field-dependence of the magnetization and its derivative for **1** at 1.8 K. (b) Temperature-dependence (from 1.8 to 7 K) of the magnetic susceptibility for **1** at different fields from 100 to 15000 G.

If antiferromagnetic inter-dimer exchange is clearly relevant in **1**, zero-field splitting effects originating from the single Mn(III) ion anisotropy is also an important contribution to understand the decrease of the susceptibility at low temperature in **1** and even more so in the other compounds. Therefore, the magnetic susceptibility for **2**–**4** and **6** can be modelized by the dimer equation for two equivalent $S = 2$ ($S_1 = S_2 = S$) magnetic spins including the ZFS term D. The following Hamiltonian was used:[11,19,20]

$$\boldsymbol{H} = 2g\mu_B HS - 2JS_1\cdot S_2 + 2D[S^2_z - 1/3S(S+1)] \quad (1)$$

where J is the intra-dimer magnetic exchange, D the zero-field splitting (ZFS) originating from each Mn(III) ion. Intermolecular interactions were not included in the fitting of the compounds with large inter-dimer distances (**2**–**4** and **6**), this structural feature vouching for these interactions being negligibly small. For **1**, inter-dimer interactions ($zJ' \approx -0.8$ cm^{-1}) were introduced by the molecular field approximation in order to fit the magnetic susceptibility. The best-fitting parameters obtained for **1**–**4** and **6** are summarized in Table 2. The intra-dimer interaction parameter J for all compounds is found to be positive, indicating ferromagnetic interaction between manganese(III) ions through phenolate oxygen. The ZFS term D is estimated to be in the negative range from −0.38 to −2.53 cm^{-1} which is consistent with the typical value of Mn(III)–salen analogues and with Jahn–Teller distortion (*vide infra*).[11]

Interestingly, compound **5** exhibits a very weak ferromagnetic interaction revealed in the low temperature region of the magnetic susceptibility (see Fig. 6). The temperature dependence of χT has a weak maximum at 8.0 K and then decreases at lower temperature. Knowing the monomeric nature of the Mn(III) complex in **5**, this feature can only be due to ferromagnetic inter-molecular interactions. Magnetic susceptibility data of **5** were fitted to an isolated S = 2 magnetic spin with a ZFS term D using the following spin Hamiltonian:[11]

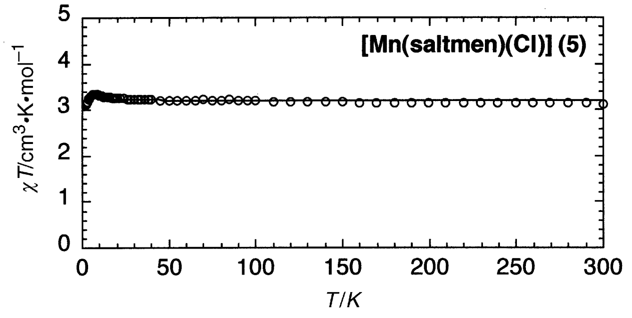

Fig. 6 χT *vs.* T plot of **5**. The solid line represents the best fit obtained using the parameters summarized in Table 2.

$$\boldsymbol{H} = g\mu_B HS + D[S^2_z - 1/3S(S+1)] \quad (2)$$

To take into account the ferromagnetic inter-dimer interaction a molecular field exchange parameter zJ' was added to the model. In spite of being very small therefore not very accurate, the obtained zJ' value is positive, +0.05 cm^{-1}, confirming the presence of weak ferromagnetic interaction. The decrease of χT at low temperature region is associated with the ZFS of Mn(III) ion which is found to be −1.60 cm^{-1}.

Discussion on correlation between structure and magnetic behavior

Although several out-of-plane dimeric manganese(III)–salen-type compounds have been reported so far, only four compounds exhibiting ferromagnetic interaction have been described.[2b,12–14] Table 2 summarized the pertinent bond distances and angles of the dimeric cores and the estimated magnetic parameters. Bridging angles of all compounds are

Table 2 Pertinent bond distances (Å) and angles (°) for the out-of-plane dimeric cores and magnetic parameters obtained from the best fitting of the magnetic susceptibility (F = ferromagnetic Interaction, AF = antiferromagnetic interaction)

							Magnetic parameters				
	Mn–O	Mn–O*	O–Mn–O*	Mn–O–Mn*	Mn ··· Mn*		*g*	J/cm^{-1}	D/cm^{-1}	zJ/cm^{-1}	Ref.
1	1.909(2)	2.434(2)	78.42(10)	101.58(10)	3.381(1)	F	1.93	1.79	−2.53	−0.79	This work
2	1.896(3)	2.662(3)	79.4(1)	100.6(1)	3.541(1)	F	1.96	1.20	−0.38		This work
3	1.872(2)	3.441(2)	83.76(8)	96.24(8)	4.0923(8)	F	1.99	0.55	−1.25		This work
4	1.877(2)	3.758(3)	83.43(10)	96.57(10)	4.3885(9)	F	2.03	0.12	−1.00		This work
6	1.892(5)	3.505(5)	85.8(2)	94.2(2)	4.102(2)	F	2.04	0.38	−1.87		This work
[a]	1.90(1)	2.85(1)	79.9(5)	100.1(5)	3.693(6)	F					2*b*
[b]	1.904(3)	2.627(3)	81.1(1)	98.9(1)	3.475(2)	F	2.01	1.50		−0.35	12
[c]	1.878(9)	3.103(5)	88.9(2)	91.1(2)	3.658(2)	F					13
[d]	1.901(5)	2.412(6)	79.42(21)	100.58(22)	3.334(3)	F	2.0	6.30	−1.70		14
[e]	1.912(3)	2.305(2)	76.6(1)	103.4(1)	3.318(1)	AF		−1.68			6
[f]	1.906(6)	2.419(7)	—	—	3.350(3)	AF					8
[g]	1.891(3)	2.490(3)	80.7(1)	99.3(1)	3.361(2)	AF					9
[h]	1.880(6)	2.750(6)	81.3(2)	98.7(2)	3.558(3)	AF					10*a*, 11

[a] $[Mn(saltmen)]_4[Fe(CN)_6]ClO_4$. [b] [Mn(naphtmen)(TCEA)] (TCEA = tricyanoethenolate). [c] $[Mn(salen)Cu(A)]BPh_4$ (H_2A = 4-(6-methyl-8-oxo-2,5-diazanonane-1,5,7-trienyl)imidazole). [d] $[Mn(salen)(H_2O)]_2(ClO_4)_2$. [e] $[Mn(L)(H_2O)]_2(ClO_4)_2$ (L = *N*-(acetylacetonylidene)-*N′*-(α-methylsalicylidene)-ethylenediamine). [f] $[Mn_2(bsalen)_2(H_2O)_2](ClO_4)_2$ (bsalen = *N*,*N′*-ethylenebis(5-bromosalicylideneiminato) dianion. [g] $[Mn(salen)(H_2O)]_2(ClO_4)_2{\cdot}H_2O$. [h] [Mn(salen)(NCS)].

similar to one other due to the relative rigidity of the planar ligands. On the other hand, the Mn ··· O* distances of the ferromagnetic interacting dimers are relatively longer compared with those of the antiferromagnetic compounds. Interestingly, the dimeric Mn(III) compounds with $saltmen^{2-}$ and $naphtmen^{2-}$ ligands, **1**–**4**, **6a**–**c**, show in all cases ferromagnetic interaction. Such ferromagnetic exchange can be understood by considering the arrangement of Mn(III) ion d-orbitals. The electronic configuration of the Mn(III) ion in an elongated Jahn–Teller distortion is known to be $(d_{xy})^1$, $(d_{yz})^1$, $(d_{xz})^1$ and $(d_{z^2})^1$ with a $^5B_1$ ground state.[21] The methyl group of $saltmen^{2-}$ and $naphtmen^{2-}$ acts as electronic donor and enhances the Jahn–Teller orbital splitting. Thus the ferromagnetic exchange interaction between Mn(III) ions could be mainly the result of the d_{z^2} and the dπ orbitals (d_{xy}, d_{yz} and d_{xz} orbitals) orthogonality. The correlation between the Mn ··· O* distance and the magnetic exchange parameter J_F (cm^{-1}) was observed in the Mn(III) compounds with $saltmen^{2-}$ and $naphtmen^{2-}$, **1**–**4** and **6**, as shown in Fig. 7.

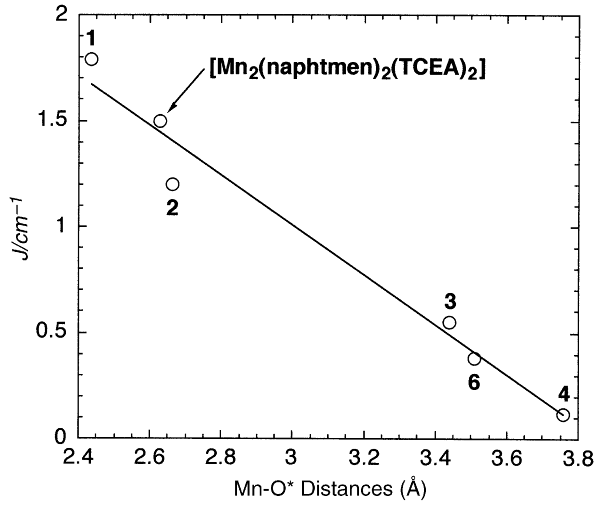

Fig. 7 Correlation between the ferromagnetic exchange parameters J_F and the Mn–O* distances in Mn(III) out-of-plane dimers with $saltmen^{2-}$ and $naphtmen^{2-}$.

Within the Mn ··· O* bond range of 2.4–3.7 Å, which is restricted to the Mn(III) dimers with $saltmen^{2-}$ and $naphtmen^{2-}$, the approximate ferromagnetic exchange parameter J_F in the out-of-plane dimeric core could be empirically estimated by the following equation:

$$J_F = 4.5724 - 1.1868x \qquad (3)$$

(x: Mn ··· O* distance (Å) in the range of 2.4–3.7 Å)

Upon increasing the Mn ··· O* distance, the ferromagnetic interaction in the out-of-plane dimeric core decreases and the exchange interaction could vanish when the Mn ··· O* distance reaches *ca.* 3.8 Å. Another important point to mention concerning orbital consideration, is probably the work of Gerritsen and Sabinsky. They have experimentally demonstrated that the anisotropy of a Mn(III) ion (ZFS term) depends significantly on this Jahn–Teller distortion. As observed in our report, they shown that an elongated Jahn–Teller distortion leads to a negative ZFS paramater.[22]

In summary, we have reported synthesis, structure analysis and magnetic properties of new Mn^{III}_2 cores. These new building blocks exhibit intra-dimer ferromagnetic exchange that is influenced by subtle geometric and electronic factors. The use of $saltmen^{2-}$ and $naphtmen^{2-}$ ligands confers to these dimeric units an $S = 4$ spin ground state and then the possibility to afford interesting polymeric architectures by connecting them to other magnetic units. As a precursor example, the 2-D compound $\{[\{Mn(saltmen)\}_4\{Fe(CN)_6\}]^+\}_n$ includes a Mn(III) dimeric linkage.[2b] This material has been reported to be a ferromagnet below 4 K. For this system, the ferromagnetic exchanges, in the Mn(III) out-of-plane dimeric core and between Mn(III) ion and low spin Fe(III) ion, produced a tri-dimensional magnetic ordering. The association of the new $S = 4$ building blocks reported in the present paper to other magnetic units seems to be promise a interesting future for the design of new molecule-based magnetic materials.

Acknowledgements

This work was supported by a grant from the JSPS Research Fellowships for Young Scientists and partly from "Structural Ordering and Physical Properties", PRESTO, Japan Science and Technology Corporation (JST) (H. M.).

References and notes

1 Reviews: (*a*) O. Kahn, *Molecular Magnetism*, VCH, Weinheim, Germany, 1993; (*b*) O. Kahn, *Struct. Bonding (Berlin)*, 1987, **68**, 89; (*c*) J. S. Miller and A. J. Epstein, *Angew. Chem., Int. Ed. Engl.*, 1994, **33**, 385; (*d*) D. Gatteschi, *Adv. Mater.*, 1994, **6**, 635.

2 (*a*) H. Miyasaka, N. Matsumoto, H. Okawa, N. Re, E. Gallo and C. Floriani, *Angew. Chem., Int. Ed. Engl.*, 1995, **34**, 1446; (*b*) H. Miyasaka, N. Matsumoto, H. Okawa, N. Re, E. Gallo and

C. Floriani, *J. Am. Chem. Soc.*, 1996, **118**, 981; (*c*) N. Re, E. Gallo, C. Floriani, H. Miyasaka and N. Matsumoto, *Inorg. Chem.*, 1996, **35**, 6004; (*d*) H. Miyasaka, N. Matsumoto, N. Re, E. Gallo and C. Floriani, *Inorg. Chem.*, 1997, **36**, 670; (*e*) H. Miyasaka, H. Ieda, N. Matsumoto, N. Re, R. Crescenzi and C. Floriani, *Inorg. Chem.*, 1998, **37**, 255; (*f*) H. Miyasaka, H. Okawa, A. Miyazaki and E. Toshiaki, *Inorg. Chem.*, 1998, **37**, 4878; (*g*) H. Miyasaka, H. Okawa, A. Miyazaki and E. Toshiaki, *J. Chem. Soc., Dalton Trans.*, 1998, 3991.

3 Manganese(III) salen-type Schiff base compounds are in equilibrium between the monomeric species $[Mn(L)(H_2O)(S)]^+$ (**A**) and the dimeric species $[Mn_2(L)_2(H_2O)_2]^{2+}$ (**B**) (L = salen-type Schiff base ligand, S = unidentate solvent ligand) in solution, and the solid-state form depends on the steric characteristics of the salen-type Schiff base ligand, used solvent, and donor-activity of coordination-donor species (solvent or other ligand).

4 Y. Cringh, S. W. Gordon-Wylie, R. E. Norman, G. R. Clark, S. T. Weintraub and C. P. Horwitz, *Inorg. Chem.*, 1997, **36**, 4968.

5 C. E. Hulme, M. Watkinson, M. Haynes, R. G. Pritchard, C. A. McAuliffe, N. Jaiboon, B. Beagley, A. Sousa, M. R. Bermejo and M. Fondo, *J. Chem. Soc., Dalton Trans.*, 1997, 1805.

6 N. Matsumoto, Z. J. Zhong, H. Okawa and S. Kida, *Inorg. Chim. Acta*, 1989, **160**, 153.

7 N. Matsumoto, N. Takemoto, A. Ohyosi and H. Okawa, *Bull. Chem. Soc. Jpn.*, 1988, **61**, 2984.

8 M. R. Bermejo, A. Castiñeiras, J. C. Garcia-Monteagudo, M. Rey, A. Sousa, M. Watkinson, C. A. McAuliffe, R. G. Pritchard and R. L. Beddoes, *J. Chem. Soc., Dalton Trans.*, 1996, 2935.

9 A. Garcia-Deibe, A. Sousa, M. R. Bermejo, P. P. MacRory, C. A. McAuliffe, R. G. Pritchard and M. Hellowell, *J. Chem. Soc., Chem. Commun.*, 1991, 728.

10 (*a*) M. Mikuriya, Y. Yamato and T. Tokii, *Bull. Chem. Soc. Jpn.*, 1992, **65**, 1466; (*b*) H. Li, Z. J. Zhong, C. Duan, X. You, T. C. W. Mak and B. Wu, *J. Coord. Chem.*, 1997, **41**, 183.

11 B. J. Kennedy and K. Murray, *Inorg. Chem.*, 1985, **24**, 1552.

12 Y. Sato, H. Miyasaka, N. Matsumoto and H. Okawa, *Inorg. Chim. Acta*, 1996, **247**, 57.

13 N. Matsumoto, H. Okawa, S. Kida, T. Ogawa and A. Ohyoshi, *Bull. Chem. Soc. Jpn.*, 1989, **62**, 3812.

14 H.-L. Shyu, H.-H. Wei and Y. Wang, *Inorg. Chim. Acta*, 1999, **290**, 8.

15 E. A. Boudreaux and L. N. Mulay, *Theory and Applications of Molecular Paramagnetism*, John Wiley and Sons, New York, 1976, pp. 491–495.

16 (*a*) SIR92: A. Altomare, M. C. Burla, M. Camalli, M. Cascarano, C. Giacovazzo, A. Guagliardi and G. Polidori, *J. Appl. Crystallogr.*, 1994, **27**, 435; (*b*) PATTY: P. T. Beurskens, G. Admiraal, G. Beurskens, W. P. Bosman, S. Garcia-Granda, R. O. Gould, J. M. M. Smits and C. Smykalla, 1992; (*c*) SHELX97: G. M. Sheldrick, Program for the Solution of Crystal Structures, University of Göttingen, Germany, 1997.

17 DIRDIF94: P. T. Beurskens, G. Admiraal, G. Beurskens, W. P. Bosman, R. de Gelder, R. Israel, J. M. M. Smits. The DIRDIF program system, Technical Report of the Crystallography Laboratory, University of Nijmegen, The Netherlands, 1994.

18 teXsan: Crystal Structure Analysis Package, Molecular Structure Corporation, The Woodlands, TX, 1985 and 1992.

19 P. Garge, R. Chikate, S. Padhye, J.-M. Savariault, P. Loth and J.-P. Tuchagues, *Inorg. Chem.*, 1990, **29**, 3315.

20 R. C. Reem and E. I. Solomon, *J. Am. Chem. Soc.*, 1987, **109**, 1216.

21 M. Corbella, R. Costa, J. Ribas, P. H. Fries, J.-M. Latour, L. Öhrström, X. Solans and V. Rodrigez, *Inorg. Chem.*, 1996, **35**, 1857.

22 H. J. Gerritsen and E. S. Sabinsky, *Phys. Rev.*, 1963, **132**, 1507.